Quantum dynamics of the Walden inversion reaction Cl−+CH3Cl→ClCH3+Cl−

David C. Clary and Juliana Palma

Citation: The Journal of Chemical Physics **106**, 575 (1997); doi: 10.1063/1.473397
View online: http://dx.doi.org/10.1063/1.473397
View Table of Contents: http://scitation.aip.org/content/aip/journal/jcp/106/2?ver=pdfcov
Published by the AIP Publishing

Quantum dynamics of the Walden inversion reaction $Cl^- + CH_3Cl \rightarrow ClCH_3 + Cl^-$

David C. Clary
Department of Chemistry, University College London, 20 Gordon Street, London WC1H OAJ, United Kingdom

Juliana Palma
Centro de Estudios e Investigaciones, Universidad Nacional de Quilmes, Saenz Pena 180, 1876 Bernal, Argentina

(Received 12 August 1996; accepted 1 October 1996)

Quantum scattering calculations on the S_N2 reaction $Cl^- + CH_3Cl \rightarrow ClCH_3 + Cl^-$ are reported. The rotating bond approximation (RBA) has been adapted so that three degrees of freedom including the C–Cl stretching vibration and the CH_3 umbrella mode are treated explicitly. The calculations have been done with minor modifications of a potential due to Vande Linde and Hase. It is found that initial excitation of the C–Cl vibration has a large effect on the reaction probabilities, while excitation of the CH_3 umbrella vibration is less significant. The reaction is dominated by scattering resonances with lifetimes ranging from 0.1 to 10 ps. It is found that the length of the C–Cl bond at the transition state of the reaction has a particularly pronounced effect on the reaction probabilities. The magnitude of the quantum reaction probabilities compares quite well with those calculated using the quasiclassical trajectory method. © *1997 American Institute of Physics.* [S0021-9606(97)00602-8]

I. INTRODUCTION

The Walden inversion reaction

$$Cl^- + CH_3Cl \rightarrow ClCH_3 + Cl^-$$

is one of the classic reactions in physical organic chemistry.[1] There is strong evidence[2,3] that this S_N2 nucleophilic reaction has a potential energy surface characterized by a symmetric transition state containing a planar CH_3 group with two C–Cl bonds equal in length, and separated pre- and post-reaction ion-dipole complexes. The effect of solvent on this reaction is of great interest[4–7] but even the gas phase kinetics and dynamics are still not well understood. Of particular concern is whether the presence of the ion-dipole complexes allows statistical theories (such as RRKM and transition state theory) to be applied to this reaction or whether a detailed dynamical treatment is necessary.[1] Related to this question is the relative effect of the different vibrational and rotational modes of CH_3Cl on the reaction.[8] Although detailed reaction dynamics experiments have not yet been done on this reaction, the measured reaction rate constant is fairly small (3.5×10^{-14} cm^3 s^{-1} $molecule^{-1}$).[9]

Advances in theoretical chemistry are enabling realistic calculations on the dynamics of the $Cl^- + CH_3Cl$ reaction to be carried out. A multidimensional potential energy surface has been constructed from *ab initio* calculations of energy points by Tucker and Truhlar[10] and this potential has been used by the same authors in transition state theory calculations of rate constants. This group has also studied this reaction and similar ones using potentials based on semi-empirical theory,[11] and has considered the reaction microsolvated by water molecules.[12] Hase and co-workers have also constructed a similar potential energy surface[13] which has been used in an extensive series of quasiclassical trajectory computations on the dynamics of the unimolecular and bimolecular reaction.[1,14–18] One of the main conclusions from these studies of Hase and co-workers is that the reaction dynamics is not statistical, there being very weak coupling between the internal modes of the CH_3Cl molecule and the intermolecular modes. They found that trajectories initialized at the central barrier remain trapped close to the barrier with frequent barrier recrossings implying a bottleneck for energy transfer between the intermolecular and intramolecular modes of the complex.[1] These authors came to similar conclusions[19] in studies of the related exothermic reaction $Cl^- + CH_3Br \rightarrow CH_3Cl + Br^-$, which is a reaction that appears to have no barrier in the potential energy surface. It was suggested that theories such as RRKM and transition state theory are, therefore, not appropriate for these reactions. However, Hase *et al.* do note that there are problems with applying quasiclassical trajectory computations to reactions of this type in that zero-point energy quantization is not treated properly.

There have been some approximate quantum scattering calculations on S_N2 reactions by Basilevsky and Ryaboy.[20,21] They used a two-degree of freedom reaction path Hamiltonian model and found that scattering resonances associated with the ion-dipole complexes were important in these reactions. To date, there have been no other quantum scattering calculations on S_N2 reactions that go beyond two degrees of freedom. Clearly such calculations will be useful given the uncertainties, alluded to above, in understanding the reaction dynamics of these reactions.

There have been significant recent advances in extending quantum scattering theory to the reactions of polyatomic molecules that has followed on from the very impressive progress that has been made in performing accurate calcula-

tions on atom+diatom reactions.[22,23] The first quantum scattering calculations for a polyatomic reaction were on $H+HCN \rightarrow H_2+CN$ for linear geometry,[24,25] and these were shortly followed by computations on the $OH+H_2 \rightarrow H_2O+H$ reaction using the rotating bond approximation (RBA).[26] The RBA moved away from the linear approximation and enabled reaction cross sections to be calculated selected in the rotational quantum states of OH and the vibrational bending mode of H_2O.[27,28] More recently, other methods have been applied to the $OH+H_2$ reaction, including the reduced dimensionality approach of Bowman and co-workers,[29] time-dependent calculations by both Zhang and co-workers[30] and Neuhauser[31] that give accurate reaction probabilities selected in the initial ro-vibrational states of OH and H_2 and summed over all final states, and calculations of accurate cumulative reaction probabilities, summed over all initial and final states, of Manthe *et al.*[32] The method of Baer and co-workers that uses negative imaginary potentials (NIPS) has also been applied to this reaction with some additional approximations.[33] Accurate state-to-state reaction probabilities have also been calculated in planar geometry by Echave and Clary.[34] Several other approximate methods have also been applied recently to the $OH+H_2$ reaction.[35,36] Very recently, Zhang and Light have also reported wave packet calculations of reaction probabilities for the $H+H_2O \rightarrow OH+H_2$ reaction selected in certain reactant and product states.[37]

Given this progress in performing quantum reactive scattering calculations on the $OH+H_2$ reaction, it is important to extend the theory to other reactions involving polyatomics. The RBA has been applied to several such reactions, including[38–42] $OH+CO \rightarrow H+CO_2$, $OH+HCl \rightarrow H_2O+Cl$, $OH+HBr \rightarrow H_2O+Br$, $H+HCN \rightarrow H_2+CN$, $OH+CH_4 \rightarrow H_2O+CH_3$, and $OH+NH_3 \rightarrow H_2O+NH_2$. Also the reduced dimensionality method of Bowman has been applied to $H+C_2H_2 \rightarrow H_2+C_2H$[43] and the NIPS method of Baer *et al.* has been used in approximate calculations of cumulative reaction probabilities for the reaction $O+O_3 \rightarrow O_2+O_2$.[44] Very recently, the OH+CO reaction has been the subject of time-dependent calculations by Goldfield *et al.*[45] (for planar geometry) and Zhang and co-workers (for five degrees of freedom).[46]

In this paper we describe how the RBA can be adapted to calculate state-to-state reaction probabilities and cross sections for the Walden inversion reaction

$$Cl^- + CH_3Cl(m,n) \rightarrow ClCH_3(m',n') + Cl^-,$$

where m and n refer to quantum numbers that label the CH_3 umbrella and C–Cl stretching vibrational modes, respectively. We use potentials adapted from the analytical multidimensional potential of Hase and co-workers[13] that is based on *ab initio* data. One aim of our study is to examine how excitation in the CH_3 umbrella mode affects the reaction probabilities: since the reaction involves an inversion of this mode it might be thought that it should significantly influence the reaction dynamics. We also examine the importance of the topology of the potential energy surface on the reaction and find that the length of the C–Cl bond at the transition state of the reaction is particularly significant. Since the potential energy surface has two deep wells that allow the formation of long-lived complexes, it is also of interest to examine the effect of quantum resonances on the chemical reaction.

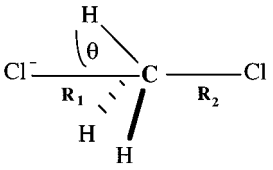

FIG. 1. Coordinates for the RBA calculation on the $Cl^- + CH_3Cl$ interaction.

This paper is organized as follows. In Sec. II we describe how the RBA can be adapted to calculate reaction probabilities, cross sections, and rate constants for the Walden inversion reaction. Section III describes the modifications we have made to the potential energy surface of Hase and co-workers to examine how the reaction probabilities relate to the topology of the surface. Quasiclassical trajectory (QCT) calculations that we have performed for comparison with the quantum calculations are reported in Sec. IV. Results are described in Sec. V and conclusions are made in Sec. VI.

II. ROTATING BOND APPROXIMATION

We describe how the rotating bond approximation is adapted to the $Cl^- + CH_3Cl(m,n) \rightarrow ClCH_3(m',n') + Cl^-$ reaction. The vector joining the reactant Cl^- to the center of mass of the CH_3Cl molecule is $\mathbf{R}_1$, while the vector joining the C and Cl atoms is $\mathbf{R}_2$ (see Fig. 1). Based on the potential surface calculations and trajectory results of Hase and co-workers,[15–17] and our previous calculations on other reactions,[24,26,28] we assume that the length of the CH bonds is held fixed to R_{CH} during the reaction as these act as spectator bonds. Furthermore, as the geometry of the minimum energy path has $\mathbf{R}_1$ and $\mathbf{R}_2$ aligned, we assume this geometry for the reaction. Each CH bond has a common angle of θ with respect to the Cl–C–Cl symmetry axis and this is the ''active'' degree of freedom that enables the umbrella mode to be described. These simplifications reduce the problem to one of three degrees of freedom, with the two C–Cl bonds and the CH_3 umbrella vibration treated explicitly by θ. If necessary, all the degrees of freedom neglected in this approximation can be treated approximately by using a reduced dimensionality approximation along the lines applied by Bowman and co-workers[47] in which the potential energy surface is corrected by zero-point energies for all the modes not treated explicitly in the calculation.

With the above approximations the three degree of freedom Hamiltonian is

$$H = -\frac{\hbar^2}{2M_1}\frac{\partial^2}{\partial R_1^2} - \frac{\hbar^2}{2M_2}\frac{\partial^2}{\partial R_2^2} + Bj^2 + V(R_1,R_2,\theta), \quad (1)$$

where

$$M_1=[(m_{\mathrm{Cl}}m_{\mathrm{CH_3Cl}})/(m_{\mathrm{Cl}}+m_{\mathrm{CH_3Cl}}),$$

$$M_2=m_{\mathrm{Cl}}m_{\mathrm{CH_3}}/(m_{\mathrm{Cl}}+m_{\mathrm{CH_3}}),$$

$$M_3=m_{\mathrm{H}}m_{\mathrm{C}}/(m_{\mathrm{H}}+m_{\mathrm{C}}),$$

$$m_{\mathrm{CH_3}}=m_{\mathrm{C}}+3m_{\mathrm{H}}, \quad m_{\mathrm{CH_3Cl}}=m_{\mathrm{Cl}}+m_{\mathrm{CH_3}},$$

$$B=\frac{\hbar^2}{6M_3R_{\mathrm{CH}}^2}, \tag{2}$$

$$j^2=-\frac{1}{\sin\theta}\frac{\partial}{\partial\theta}\sin\theta\frac{\partial}{\partial\theta}, \tag{3}$$

V is the potential energy surface, and m_{C}, m_{H}, and m_{Cl} are the masses of the C, H, and Cl atoms, respectively.

It is advantageous to transform to the polar (hyperspherical) coordinates:

$$s_i^2=\frac{M_i}{\mu}R_i^2, \quad i=1 \text{ and } 2,$$

with

$$s_1=\rho\cos(\delta), \quad s_2=\rho\sin(\delta),$$

and $\mu=(M_1M_2m_{\mathrm{Cl}})^{1/3}$ and the wave function is scaled by $1/\rho^{3/2}$. The Hamiltonian is then

$$H=-\frac{\hbar^2}{2\mu}\frac{\partial^2}{\partial\rho^2}-\frac{\hbar^2}{2\mu\rho^2}\frac{\partial^2}{\partial\delta^2}+Bj^2+\frac{3\hbar^2}{8\mu\rho^2}+V(\rho,\delta,\theta). \tag{4}$$

This Hamiltonian can be solved using a coupled channel expansion in the variables δ and θ, with ρ as the scattering coordinate. We use the R-matrix propagator method[48] to do this, which involves splitting up the hyperradius ρ into sectors with midpoints $\{\rho_i\}$. In sector i, the wave function is expanded as

$$\Psi_{k'}(\rho,\delta,\theta;\rho_i)=\sum_k^N f_{kk'}(\rho;\rho_i)\psi_k(\delta,\theta;\rho_i), \tag{5}$$

where k' is the initial quantum state label. Diagonalization of the Hamiltonian of Eq. (4) with $\rho=\rho_i$, is carried out with the basis set expansion

$$\psi_k(\delta,\theta;\rho_i)=\sum_{k_1}^{N_\delta}\sum_{k_2}^{N_\theta}c_{k_1k_2}^k(\rho_i)\psi_{k_1}(\delta;\rho_i)\psi_{k_2}(\theta;\rho_i) \tag{6}$$

to give the hyperspherical adiabats $\{E_k(\rho)\}$. As is explained below, the adiabatic wave functions $\psi_k(\delta,\theta;\rho_i)$ split into nearly degenerate pairs with wave functions localized in the reactant or product channel. The size of the tunneling splitting indicates the degree of mixing between the corresponding vibrational states in the two channels for particular values of ρ.[49] In turn, this reflects the reactivity: a very small tunneling splitting for all values of ρ indicates very low reaction probabilities.

The functions $\{\psi_{k_1}(\delta;\rho_i)\}$ are obtained from diagonalization of the Hamiltonian:

$$H=-\frac{\hbar^2}{2\mu\rho_i^2}\frac{\partial^2}{\partial\delta^2}+V_0(\delta;\rho_i), \tag{7}$$

with a basis set of n_δ distributed Gaussian functions[50] on an equally spaced grid in δ. An appropriate potential $V_0(\delta;\rho_i)$ is obtained by minimizing $V(\rho_i,\delta,\theta)$ with respect to θ for each value of δ. For the title reaction this gives a symmetric double-minimum potential in δ with wells on either side corresponding to the C–Cl vibrations in reactant and product channels.

We use a basis set of n_θ normalized Legendre polynomials to diagonalize

$$H=Bj^2+V_1(\theta;\rho_i), \tag{8}$$

to give $\{\psi_{k_2}(\theta;\rho_i)\}$ where

$$V_1(\theta;\rho_i)=\langle\psi_1(\delta;\rho_i)|V(\rho_i,\delta,\theta)|\psi_1(\delta;\rho_i)\rangle. \tag{9}$$

For large ρ_i, the eigenfunctions $\psi_k(\delta,\theta;\rho_i)$ separate into doubly degenerate pairs with energies corresponding to the asymptotic (m,n) states of umbrella and C–Cl stretch vibrations, respectively, in both reactant and product channels. Examination of the sign of the expectation value

$$\langle\psi_k(\delta,\theta;\rho_i)|\cos(\theta)|\psi_k(\delta,\theta;\rho_i)\rangle$$

for large ρ enables the channels to be assigned to the reactant $(\mathrm{Cl^-}+\mathrm{CH_3Cl})$ or product $(\mathrm{CH_3Cl}+\mathrm{Cl^-})$ channels. The S-matrix elements $S_{mn,m'n'}(E)$ for collision energy E are then obtained by applying standard scattering boundary conditions.[51] The square of these S-matrix elements gives the state-selected reaction probabilities $P_{mn,m'n'}(E)$. Summation of these over all product (m',n') states gives $P_{mn}(E)$ and summing these over (m,n) gives the RBA total reaction probabilities $P(E)$. When there is significant resonance structure in the reaction probabilities, it is also possible to calculate ''smoothed'' reaction probabilities by averaging the $P(E)$ over a small energy range (e.g., 0.005 eV was used here).

It is also possible to calculate RBA cross sections by adding the centrifugal term

$$\frac{\hbar^2J(J+1)}{2\mu\rho^2}$$

to the Hamiltonian of Eq. (4) and repeating the close-coupling calculations for different values of J (but with the same adiabatic basis functions) to give the S-matrix elements $S^J_{mn,m'n'}(E)$.[26] From these the RBA state-selected integral reaction cross sections

$$\sigma(mn\rightarrow m',n')=\frac{\pi}{k_{mn}^2}\sum_J(2J+1)|S^J_{mn,m'n'}(E)|^2 \tag{10}$$

are calculated. Summation over the product $m'n'$ states gives $\sigma(mn)$.

The rotational motion of $\mathrm{CH_3Cl}$ can be treated by using an ''adiabatic bend'' procedure[52,53] that follows the approach of Bowman and co-workers,[47] or by the simpler but more approximate approach of correcting the collision energy with the bending energy of the complex at the transition state.[54,55]

This latter approach (together with the transition state vibrational frequencies reported by Vande Linde and Hase[13]) is used in some of the calculations reported here to estimate rate constants. The RBA cross sections then correspond to cross sections summed over all initial and final rotational states of the CH_3Cl for a given total energy. Boltzmann averaging of these cross sections and dividing by the rotational partition function for CH_3Cl then gives an estimate of the rate constant[55] which can be compared with experiment and other calculations.

III. POTENTIAL ENERGY SURFACES

The calculations were done with the potential energy surface of Vande Linde and Hase[13] (called V_1). This surface has a well depth for the ion-dipole complex of -10.32 kcal/mol and a barrier height of 3.6 kcal/mol at a symmetric C–Cl bond length of $r=2.38$ Å at the transition state of the reaction. The umbrella vibration changes its frequency from the asymptotic value of 1574 cm^{-1} to 1190 cm^{-1} at the transition state at which the CH_3 group is planar. This potential is quite similar to that of Tucker and Truhlar (TT)[10] whose potential is based on a similar level of *ab initio* theory (MP2/6-31G**), although the TT potential had $r=2.302$ Å.

For reasons explained in the next section, calculations were also done with a very simple modification of the V_1 potential in which the value of r was varied without changing other characteristics of the transition state such as the barrier height or the vibrational frequencies. This was done in the call to the potential by scaling the Cl–C(a) and C–Cl(b) bond distances with the Gaussian function

$$a=a(1+g\ \exp(-2(a-b)^2),$$
$$b=b(1+g\ \exp(-2(a-b)^2), \tag{11}$$

where g is a constant. The form of this function ensures that a and b are only scaled near the transition state and not elsewhere. Several *ab initio* calculations of r for the Cl^-+CH_3Cl reaction are shown in Table I. The most accurate of these calculations gives an r value close to 2.3 Å. The *ab initio* potential V_1 had $r=2.38$ Å, while potential V_2 with $g=0.04$ gives $r=2.30$ Å.

In the RBA calculations, the parameters used were $N=50$, $N_\delta=199$, $N_\theta=28$, $n_\delta=18$, and $n_\theta=28$, with boundary conditions being applied between $\rho=57$ a.u. and 150 a.u.

TABLE I. Some representative quantum chemistry calculations values of the C–Cl bond distance (r) at the transition state of the Cl^-+CH_3Cl reaction.

Authors	Geometry optimization method	r (Å)
Tucker and Truhlar, (Ref. 3)	MP2/6-31+$G(d)$	2.32
Glukhovtsev *et al.* (Ref. 61)		
Vande Linde & Hase (Ref. 13)	6-31G+MP4	2.38
Tucker and Truhlar (Ref. 10)	MP2/6-31G**	2.30
Truong & Stefanovich (Ref. 62)	BH&HLYP	2.35
Seeger (Ref. 63)	CEPA-1/$avtz$	2.32

in the way described previously.[51] Calculations were done on a very narrow energy grid (0.0001 eV) from threshold up to energies well above the barrier height to ensure that the many resonances were detected.

IV. TRAJECTORY CALCULATIONS

We performed the quasiclassical trajectory (QCT) calculations with the general chemical dynamics computer program VENUS.[56] We use the potential energy surface V_1.[10] This surface is the same as used in some of the quantum RBA calculations.

We selected the initial conditions for the trajectories using the standard options of VENUS. All trajectories were run with zero impact parameter and zero initial rotational energy. Three or four quanta of vibrational energy were given to the C–Cl stretching mode. Zero-point energy was put in the CH_3 deformation modes and no energy was added to the other modes.

The orientation of the CH_3Cl with respect to the Cl^- was selected at random. The initial separation between the Cl^- and the center of mass of the CH_3Cl was set to 30 Å for all values of the relative energy. In order to check this value of the initial separation, we ran three sets of 100 trajectories with 30, 50, and 75 Å of initial separation, respectively. Three quanta were put in the C–Cl stretching mode and 0.4 eV was put in the relative motion. We found no significant differences among the reaction probabilities calculated for the different sets.

We used the combined Runge–Kutta and Adams–Moulton algorithms in VENUS to integrate the equations of motion. Two hundred trajectories were run for each translational energy. The stepsize was set to 2×10^{-16} s. It has been shown that this stepsize is in the acceptable range for the system we are considering here.[15] The trajectories were analyzed for S_N2 substitution. A maximum integration time was set to 10 ps. It was observed that, in some trajectories, the $Cl–CH_3Cl^-$ and $ClCH_3–Cl^-$ complexes did not dissociate within this maximum integration time. These trajectories were considered as nonreactive for S_N2 substitution.

V. RESULTS

Figure 2 plots the total reaction probabilities $P(E)$ for the potentials V_1 and V_2. The first striking aspect of these plots are the large number of quantum scattering resonances. The vibrationally adiabatic barrier (VAB) in the potential is 0.10 eV and some of the reaction probability peaks do become close to unity for both potentials for collision energies above this value. Figure 3 shows plots of smoothed reaction probabilities obtained by averaging all the $P(E)$ in sectors with the range of 0.005 eV. This plot clearly shows that the average probabilities for the V_2 potential are significantly larger than those for the V_1 potential, especially at lower energies. Note also that the reaction probabilities are also quite large for some resonance energies below the VAB, thus illustrating the effect of ''corner-cutting'' on the potential energy surface that arises with the particular heavy mass ratios of this reaction.

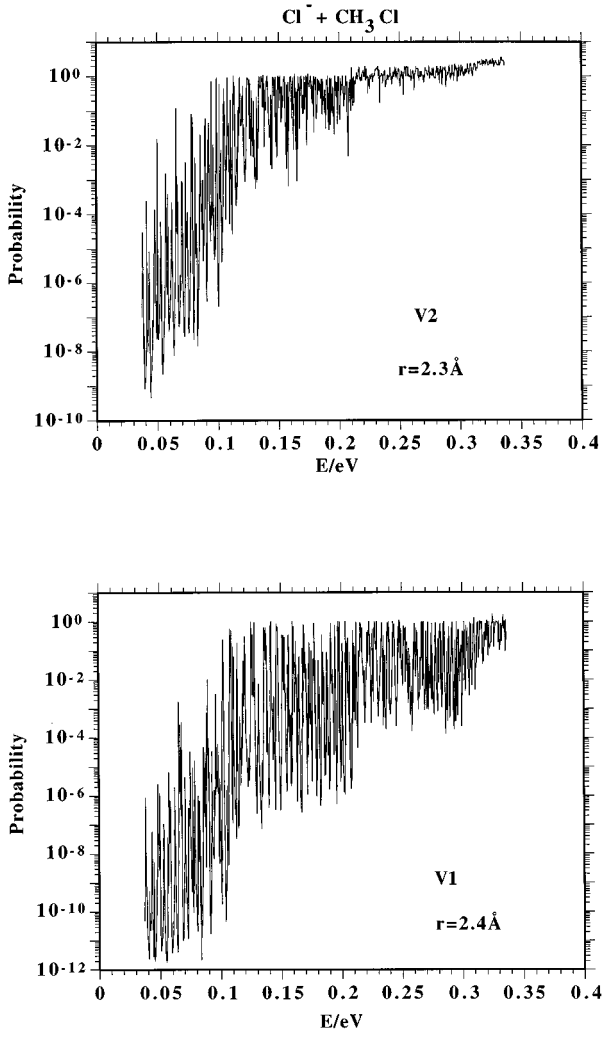

FIG. 2. Total reaction probabilities $P(E)$ for the $Cl^- + CH_3Cl$ reaction on the potential energy surfaces V_1 (lower panel with $r = 2.4$ Å) and V_2 (upper panel with $r = 2.3$ Å). E is the translational energy with respect to the ground vibrational state of CH_3Cl.

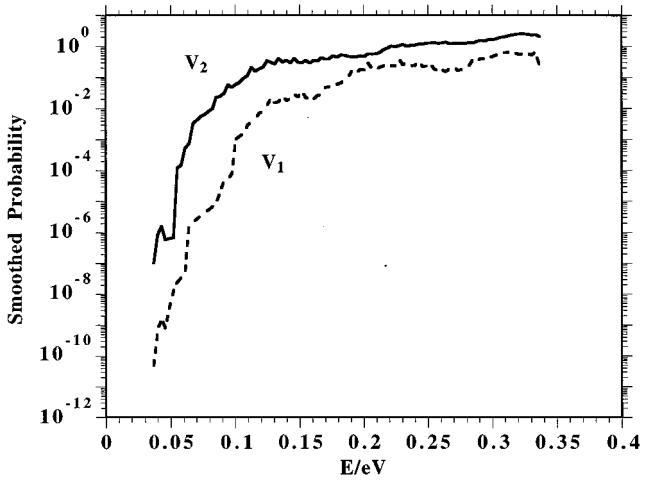

FIG. 3. Same as for Fig. 2, but reaction probabilities are smoothed over those calculated in each 0.01 eV energy interval.

It should be emphasized that both the V_1 and V_2 potentials have the same reaction and product energetics, barrier height, and vibrational frequencies at the transition state to the reaction. The only difference is the position of the transition state with respect to the length of the C–Cl bond. If transition state theory is accurate for this system, the reaction probabilities for these two potentials should essentially be identical. However, as has been emphasized by Hase using the language of classical mechanics,[1] transition state theory can break down when there is significant recrossing of trajectories in the transition state region and this is the case in their quasiclassical trajectory calculations with the V_1 potential. This recrossing of trajectories is connected with the possibility of long-lived complexes being formed in the potential wells on either side of the transition state. Furthermore, the Feshbach scattering resonances calculated in quantum mechanics are associated with excited states in these potential wells.

The RBA reaction probabilities were turned into rate constants by using the reduced dimensionality procedures, together with the vibrational frequencies of the transition state as explained in Sec. II. The rate constants obtained at 298 K are reported in Table II for the V_1 and V_2 potentials respectively, and compared with experiment.[9] Application of a microcanonical version of transition state theory (TST), in which the RBA reaction probabilities were substituted by values of unity for values of the translational energy above the vibrationally adiabatic barrier height and zero otherwise, gives the TST rate constants quoted in Table II. Note that these TST rate constants are the same for both the V_1 and V_2 potentials.

It can be seen from these results that transition state theory is overestimating the rate constants for the two potentials V_1 and V_2 (with the overestimation being most significant for V_1). Hase and co-workers also came to this conclusion from results based on their quasiclassical trajectory computations[1] on both the $Cl^- + CH_3Cl$ and $Cl^- + CH_3Br$ reactions. Our results also show that the breakdown of transition state theory is strongly connected with the length of the C–Cl bond at the transition state. Generally, sophisticated forms of transition state theory have given quite good results for simple atom+diatom reactions when compared with rate constants obtained from accurate quantum scattering calculations,[57] but it is possible that transition state theory

TABLE II. Calculations of the rate constants for the $Cl^- + CH_3Cl$ reaction at 298 K.

Method	Potential	Rate constant ($cm^3\ s^{-1}\ molec^{-1}$)
RBA	V_1	2.5×10^{-15}
RBA	V_2	1.3×10^{-14}
TST[a]	V_1	5.6×10^{-14}
TST	V_2	5.6×10^{-14}
Experiment (Ref. 9)		3.5×10^{-14}

[a]See Sec. V for a discussion of how these microcanonical TST results were calculated.

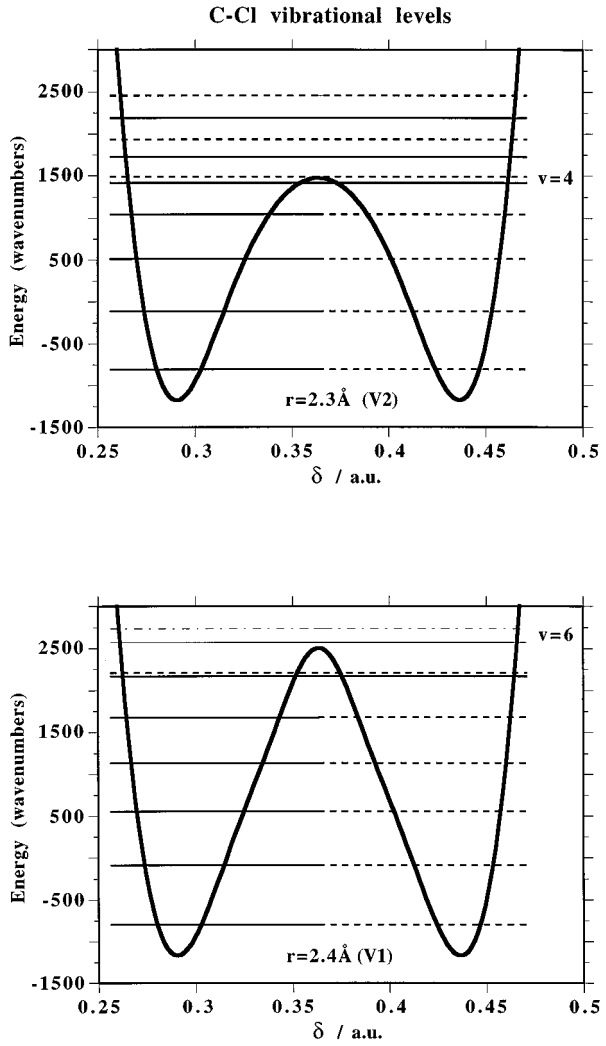

FIG. 4. Plot of $V_0(\delta;\rho)$ against $\cos(\delta)$ for the potentials V_1 (lower panel) and V_2 (upper panel) with $\rho=72$ a.u. Also shown are the low-lying hyperspherical adiabat energies $\{E_k(\rho)\}$.

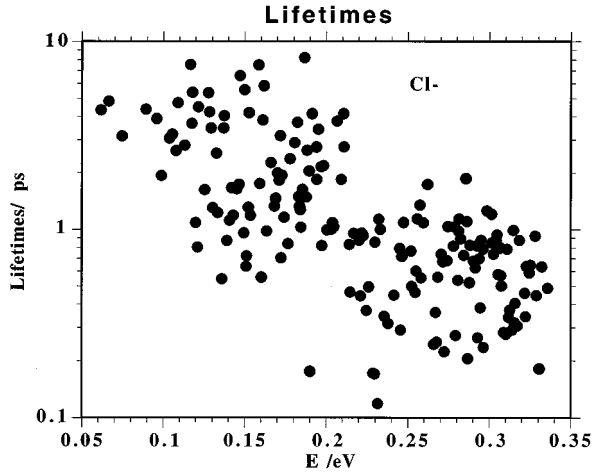

FIG. 5. Lifetimes of the scattering resonances identified for the $Cl^- + CH_3Cl$ reaction with the V_2 potential. E is the initial translational energy.

will not be so successful for reactions such as the one considered here that have deep wells in the potential either side of the reaction barrier. However, more accurate quantum mechanical scattering calculations, including more degrees of freedom, with more accurate potentials (particularly in the value of r), will be needed for a definitive test on the applicability of transition state theory to this type of reaction.

An explanation of the origin of the scattering resonances (and the importance of r) comes from examining plots of the hyperspherical potentials $V_0(\delta;\rho_i)$ of Eq. (7), together with the hyperspherical adiabats $\{E_k(\rho)\}$. Tunneling splittings between the states correlating with particular vibrations in reactants and products indicate directly the degree of reactivity that is expected:[49] a large tunneling splitting implies strong mixing between the vibrational states in reactants and products and significant reactivity. Such plots are displayed in Fig. 4 for a typical value of ρ (which is a value that includes the transition state when the δ coordinate is scanned). It is seen that there are more significant tunneling splittings for the V_2 potential for lower vibrational states than for V_1. In fact, we find that it is necessary to go up to C–Cl vibrational state $n=6$ to get a significant tunneling splitting for potential V_1. This explains why it is necessary to go to quite high vibrational states in the C–Cl stretching vibration to get appreciable reaction probabilities for the V_1 potential in both the quantum and classical calculations. Thus, it is the larger value of the C–Cl bond length at the transition state that forces the very small reaction probabilities out of the lower vibrational states for the V_1 potential: Reaction from the low vibrational states is essentially forbidden.

The arguments presented above are based on a pure adiabatic separation between the ρ and δ variables but reaction can still occur at scattering resonances, which refer to long-lived vibrationally excited states of the $Cl–CH_3Cl^-$ complex, even when the tunneling splittings in the hyperspherical adiabats are zero. This is also clearly demonstrated in quantum dynamics calculations on the well-studied $HO+CO \rightarrow CO_2+H$ reaction,[38,58] which also has a deep well in the potential energy surface. It is clear from Fig. 2 that many such resonances do arise in the quantum calculations of reaction probabilities and enable reaction to occur from vibrational states via ''nonadiabatic'' coupling between different vibrational states in the δ coordinate.

The lifetimes of the resonances are of particular interest nowadays as experimental methods have been developed to measure these for related reactive systems.[59] The linewidths Γ of the calculated resonances with energy E_r were obtained by fitting the Breit–Wigner function[38]

$$P(E)=\frac{a}{(E-E_r)^2+\frac{1}{4}\Gamma^2} \tag{12}$$

around the region of the peak of each resonance and the lifetimes τ were found from the uncertainty principle $\tau=\hbar/\Gamma$. Only lifetimes where a good fit to an isolated resonance were obtained are reported in Fig. 5 for the V_2 potential. It can be seen that the τ decrease in magnitude with increasing colli-

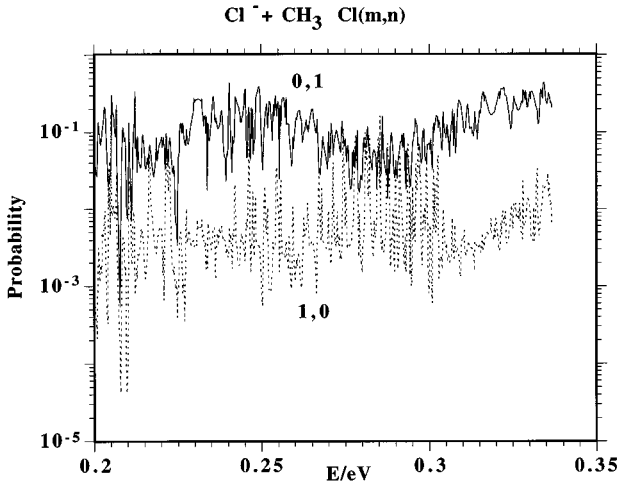

FIG. 6. Reaction probabilities P_{mn} with $(m,n)=(0,1)$ (C–Cl stretch excited) and (1,0) (CH_3 umbrella mode excited) for the potential V_1. E is the translational energy with respect to the initial vibrational state of CH_3Cl.

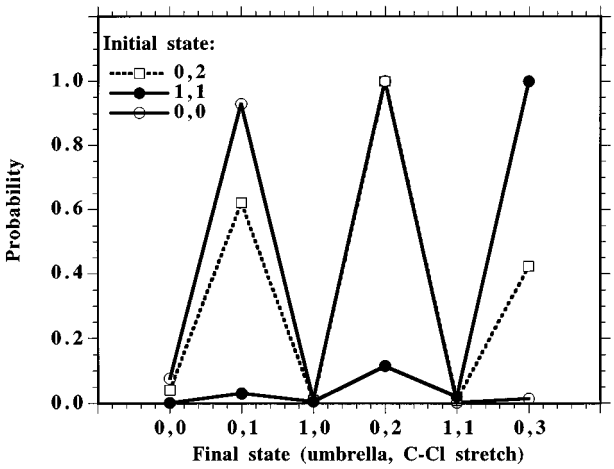

FIG. 8. State-selected RBA reaction probabilities $P(mn\rightarrow m'n')$ with $(m,n)=(0,0)$, (0,2) and (1,1) (m=umbrella, n=C–Cl stretch) for the V_1 potential. These calculations were done with a total energy of 0.32 eV with respect to the ground vibrational state of CH_3Cl. These distributions were normalized with respect to the largest probability for each individual state.

sion energy and range from 10 to 0.1 ps. This is very similar to the case of the $HO+CO\rightarrow CO_2+H$ reaction.[38,58]

Of particular interest in this study is the effect on the reaction of exciting particular initial vibrational states (m,n) in the reactant CH_3Cl. Typical results are shown in Fig. 6 for the V_1 potential in which product-summed reaction probabilities are plotted for the $(m=1,\ n=0)$ (umbrella excited) and $(m=0,\ n=1)$ (C–Cl vibration excited) initial states. It is found in our calculations on both the potentials that exciting the C–Cl vibration is significant in increasing the reaction probabilities. Excitation of the umbrella CH_3 vibration can enhance the reaction probabilities, but the overall effect of this mode is not nearly so significant. However, due to the resonance structure, there are a small number of energies for which the reaction probabilities for (1,0) are as large as those for the (0,1) initial state. Figure 7 shows ''smoothed'' reaction probabilities out of several different initial vibrational states for the V_1 potential. The effect of initial excitation of the C–Cl vibration in enhancing reaction probabilities is once again clear.

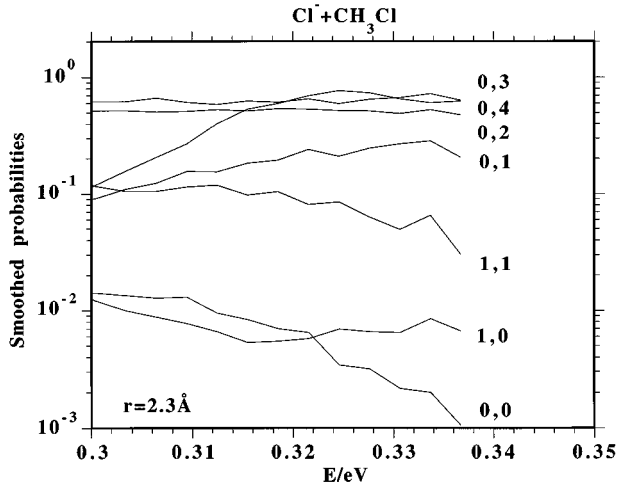

FIG. 7. Reaction probabilities P_{mn} for selected initial vibrational states of CH_3Cl (m=umbrella, n=C–Cl stretch) for the V_1 potential. These reaction probabilities are smoothed over those calculated in each 0.004 eV energy interval.

Since the CH_3 umbrella vibration deforms significantly during the reaction, and the CH_3 umbrella frequency is reduced by 25% from its asymptotic value at the transition state, it might be expected that this mode would have an even more significant influence on the reaction. Hase and co-workers also came to the conclusion in their trajectory computations that excitation of the CH_3 umbrella mode did not have a very significant effect on the reaction,[17] although these conclusions were based on an examination of large reaction cross sections on the V_1 potential and with six quanta in the initial C–Cl vibration.

Overall, these results generally confirm those we[24,26,27,38–40] and others[25,60] have found in calculations on other polyatomic reactions: Vibrational excitation of a bond being broken in a reaction can have a large effect on the reaction probability, whereas excitations of modes that are not directly broken during a reaction have a less significant effect.

Figure 8 shows typical reaction probabilities $P_{mn,m'n'}(E)$ selected in the product $m'n'$ vibrational states. It can be seen that the reaction into vibrationally excited states of the C–Cl bond is strongly favored, while the umbrella mode of the product CH_3Cl is hardly excited. This once again emphasizes the spectator nature of the umbrella mode on the reaction.

An important question that should be asked is whether the degrees of freedom ignored in the calculation (particularly the angular coordinates) would substantially change the above conclusions concerning the reactivity with the different potentials. In their quasiclassical trajectory computations, Hase and co-workers found that initial rotational excitation of the CH_3Cl molecule did not significantly effect the reac-

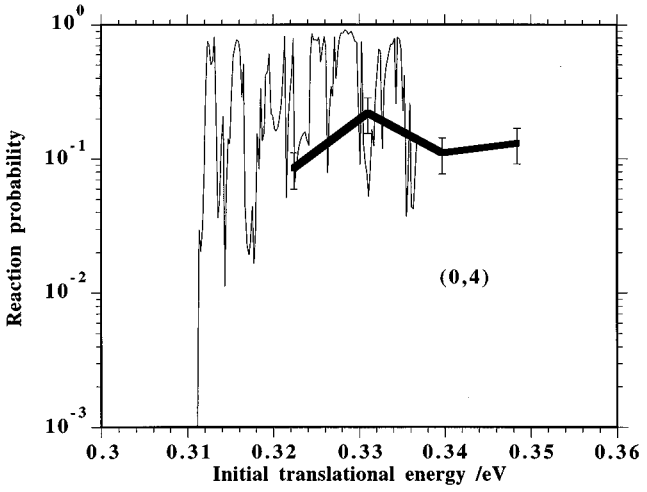

FIG. 9. Reaction probabilities P_{mn} for the (0,4) initial vibrational state of CH_3Cl for the V_1 potential. Quantum (narrow line) and QCT (broad line and error bars) results are compared.

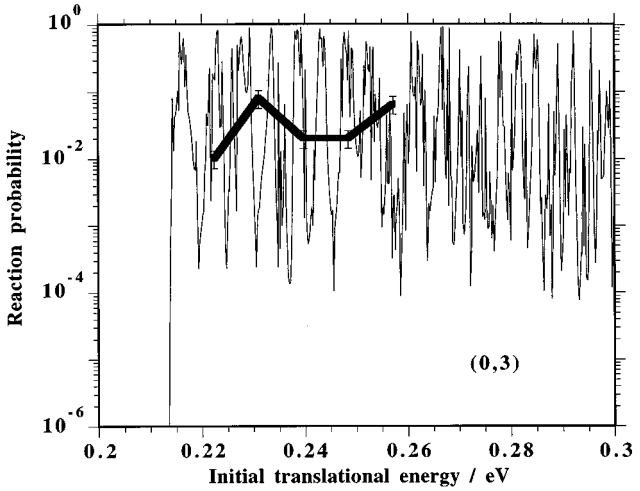

FIG. 10. Reaction probabilities P_{mn} for the (0,3) initial vibrational state of CH_3Cl for the V_1 potential. Quantum (narrow line) and QCT (broad line and error bars) results are compared.

tion cross sections that they calculated out of the $n=6$ C–Cl vibration.[17] This provides further evidence to justify the use of the RBA for a reaction such as this. However, it is possible that inclusion of other degrees of freedom and their couplings with the degrees of freedom explicitly treated in our calculation could be important, especially for the validity of transition state theory.

Figures 9 and 10 compare the RBA reaction probabilities for the reaction of Cl^- with $CH_3Cl(0,3)$ and $CH_3Cl(0,4)$ with those we calculated using the QCT method for the V_1 potential. The agreement between the absolute magnitude of the QCT and (averaged) quantum reaction probabilities is quite good, although the trajectories do not pick up the sharp resonance structures.

VI. CONCLUSIONS

Quantum scattering calculations have been carried out on the $Cl^-+CH_3Cl \rightarrow ClCH_3+Cl^-$ reaction. An adaptation of the rotating bond approximation is developed that involves the explicit treatment of three degrees of freedom including the C–Cl stretching vibration and the CH_3 umbrella mode. The calculations have been carried out with the potential (or small modification) due to Vande Linde and Hase. The potentials have a barrier with a symmetric transition state and ion-dipole complexes on either side.

Reactive scattering resonances dominate the reaction probabilities with lifetimes ranging from 10 ps to 0.1 ps as the collision energy is increased. It is found that initial excitation of the C–Cl vibration has a significant effect on the reaction probabilities, while initial excitation of the CH_3 umbrella vibration is not so important. Furthermore, excitations of the C–Cl vibration dominate the vibrational product distribution of the reaction. These findings have some similarities to those that we and others have found in calculations on a variety of polyatomic reactions: Vibrational excitation of a bond being broken or formed in a reaction has a major effect on the reaction probabilities while the effect of other spectator modes is not so significant. The agreement of the averaged magnitude of reaction probabilities with those calculated using the classical trajectory method is quite good.

The overall magnitude of the reaction probabilities is found to be very sensitive to the length r of the C–Cl bond at the transition state of the reaction. Plots of the potential energy surfaces using hyperspherical coordinates give a clear explanation of this effect. With the larger values of r, there is never any mixing between the low-lying vibrational states correlating with the reactant and product C–Cl vibrations and the tunneling splittings between the hyperspherical adiabat energies are essentially zero. This means that reaction only then occurs at energies corresponding to scattering resonances for these vibrational states.

Our conclusions are based on a quantum model that treats explicitly three degrees of freedom: the two C–Cl stretches and the CH_3 umbrella mode. Quantum scattering calculations that include the angular coordinates and the CH_3Cl rotations are the next computational improvement that is needed, and we are currently modifying the RBA in that direction. Furthermore, we have been extending the RBA to the reaction $Cl^-+CH_3Br \rightarrow ClCH_3+Br^-$. Our study also demonstrates that feasible (but approximate) quantum-dynamical calculations can now be done on reactions well beyond those containing three or four atoms.

ACKNOWLEDGMENTS

This work was supported by the Engineering and Physical Sciences Research Council, the European Union, and the British Council. D.C.C. is very grateful to W. Hase and H. Wang for sending their VENUS program that contains the potential energy surface for the Cl^-+CH_3Cl reaction and also to W. Hase, D. Truhlar, and H. Bowen for useful discussions.

[1] W. L. Hase, Science **266**, 998 (1994).
[2] W. N. Olmstead and J. I. Brauman, J. Am. Chem. Soc. **99**, 4219 (1977).

[3] S. C. Tucker and D. G. Truhlar, J. Phys. Chem. **93**, 8138 (1989).
[4] W. L. Jorgensen and J. K. Buckner, J. Phys. Chem. **90**, 4651 (1986).
[5] J. P. Bergsma, B. J. Gertner, K. R. Wilson, and J. T. Hynes, J. Chem. Phys. **86**, 1356 (1987).
[6] S. E. Huston, P. J. Rossky, and D. A. Zichi, J. Am. Chem. Soc. **111**, 5680 (1989).
[7] S. C. Tucker and D. G. Truhlar, Chem. Phys. Lett. **157**, 164 (1989).
[8] R. D. Levine and R. B. Bernstein, J. Phys. Chem. **92**, 6954 (1988).
[9] S. E. Barlow, J. M. VanDoren, and V. M. Bierbaum, J. Am. Chem. Soc. **106**, 7240 (1988).
[10] S. C. Tucker and D. G. Truhlar, J. Am. Chem. Soc. **112**, 3338 (1990).
[11] A. Gonzalez-Lafont, T. N. Truong, and D. G. Truhlar, J. Phys. Chem. **95**, 4618 (1991).
[12] S. C. Tucker and D. G. Truhlar, J. Am. Chem. Soc. **112**, 3362 (1990).
[13] S. R. Vande Linde and W. L. Hase, J. Phys. Chem. **94**, 2778 (1990).
[14] S. R. Vande Linde and W. L. Hase, J. Am. Chem. Soc. **111**, 2349 (1989).
[15] S. R. Vande Linde and W. L. Hase, J. Chem. Phys. **93**, 7962 (1990).
[16] S. R. Vande Linde and W. L. Hase, J. Phys. Chem. **94**, 6148 (1990).
[17] Y. J. Cho, S. R. Vande Linde, L. Zhu, and W. L. Hase, J. Chem. Phys. **96**, 8275 (1992).
[18] W. L. Hase and Y. J. Cho, J. Chem. Phys. **98**, 8626 (1993).
[19] H. Wang, G. H. Peslherbe, and W. L. Hase, J. Am. Chem. Soc. **116**, 9644 (1994).
[20] M. V. Basilevsky and V. M. Ryaboy, Chem. Phys. Lett. **129**, 71 (1986).
[21] V. M. Ryaboy, Chem. Phys. Lett. **159**, 371 (1989).
[22] W. H. Miller, Annu. Rev. Phys. Chem. **41**, 245 (1990).
[23] D. E. Manolopoulos and D. C. Clary, Annu. Rep. C. R. Soc. Chem. **86**, 95 (1989).
[24] A. N. Brooks and D. C. Clary, J. Chem. Phys. **92**, 4178 (1990).
[25] Q. Sun and J. M. Bowman, J. Chem. Phys. **92**, 5201 (1990).
[26] D. C. Clary, J. Chem. Phys. **95**, 7298 (1991).
[27] D. C. Clary, J. Chem. Phys. **96**, 3656 (1992).
[28] D. C. Clary, Chem. Phys. Lett. **192**, 34 (1992).
[29] J. M. Bowman and D. Wang, J. Chem. Phys. **96**, 7852 (1992).
[30] D. H. Zhang and J. Z. H. Zhang, J. Chem. Phys. **99**, 5615 (1993).
[31] D. Neuhauser, J. Chem. Phys. **100**, 9272 (1994).
[32] U. Manthe, T. Seideman, and W. H. Miller, J. Chem. Phys. **99**, 10 078 (1993).
[33] H. Szichman and M. Baer, J. Chem. Phys. **101**, 2081 (1994).
[34] J. Echave and D. C. Clary, J. Chem. Phys. **100**, 402 (1994).
[35] W. H. Thompson and W. H. Miller, J. Chem. Phys. **101**, 8620 (1994).
[36] N. Balakrishnan and G. D. Billing, Chem. Phys. Lett. **233**, 145 (1995).
[37] D. H. Zhang and J. C. Light, J. Chem. Phys. **104**, 4544 (1996).
[38] D. C. Clary and G. C. Schatz, J. Chem. Phys. **99**, 4578 (1993).
[39] D. C. Clary, G. Nyman, and R. Hernandez, J. Chem. Phys. **101**, 3704 (1994).
[40] D. C. Clary, J. Phys. Chem. **99**, 13 664 (1995).
[41] G. Nyman, J. Chem. Phys. **104**, 6154 (1996).
[42] G. Nyman and D. C. Clary, J. Chem. Phys. **101**, 5756 (1994).
[43] D. Wang and J. M. Bowman, J. Chem. Phys. **101**, 8646 (1994).
[44] H. Szichman, A. J. C. Varandas, and M. Baer, J. Chem. Phys. **102**, 3474 (1995).
[45] E. M. Goldfield, S. K. Gray, and G. C. Schatz, J. Chem. Phys. **102**, 8807 (1995).
[46] D. H. Zhang and J. Z. H. Zhang, J. Chem. Phys. **103**, 6512 (1995).
[47] J. M. Bowman, J. Phys. Chem. **95**, 4960 (1991).
[48] J. C. Light and R. B. Walker, J. Chem. Phys. **65**, 4272 (1976).
[49] J. Romelt, in *The Theory of Chemical Reaction Dynamics*, edited by D. C. Clary (Reidel, Dordrecht, 1986), p. 77.
[50] I. P. Hamilton and J. C. Light, J. Chem. Phys. **84**, 306 (1986).
[51] G. Nyman and D. C. Clary, J. Chem. Phys. **100**, 3556 (1994).
[52] E. M. Mortenson and K. S. Pitzer, Chem. Soc. Spec. Publ. **16**, 57 (1979).
[53] B. C. Garrett and D. G. Truhlar, Proc. Natl. Acad. Sci. U.S.A. **76**, 4755 (1979).
[54] S. L. Mielke, G. C. Lynch, D. G. Truhlar, and D. W. Schwenke, Chem. Phys. Lett. **216**, 441 (1993).
[55] D. C. Clary, J. Phys. Chem. **98**, 10678 (1994).
[56] W. L. Hase, R. J. Duchovic, X. Hu, K. F. Lim, D.-H. Lu, G. H. Peselherbe, K. N. Swamy, S. R. Vande Linde, H. Wang, and R. J. Wolf, *Program package* VENUS 96 (to be submitted).
[57] D. G. Truhlar, A. D. Isaacson, and B. C. Garrett, in *Theory of Chemical Reaction Dynamics*, edited by M. Baer (CRC, Boca Raton, FL, 1985), Vol. IV, p. 65.
[58] M. I. Hernandez and D. C. Clary, J. Chem. Phys. **101**, 2779 (1994).
[59] N. F. Scherer, L. R. Khundkar, R. B. Bernstein, and A. H. Zewail, J. Chem. Phys. **87**, 1451 (1987).
[60] D. G. Truhlar and A. D. Isaacson, J. Chem. Phys. **77**, 3516 (1982).
[61] M. N. Glukhovtsev, A. Pross, and L. Radom, J. Am. Chem. Soc. **117**, 2024 (1995).
[62] T. N. Truong and E. V. Stefanovich, J. Phys. Chem. **99**, 14700 (1995).
[63] S. K. Seeger, Ph.D. thesis, University of Gottingen, 1995.